

1 **Estimating Transient Climate Response in a large-ensemble global climate model simulation**

2

3 B.K. Adams and A.E. Dessler*

4 Dept. of Atmospheric Sciences, Texas A&M University, College Station, TX

5 * corresponding author, adessler@tamu.edu

6

7 Main points:

8 1. In a large model ensemble, we find that estimates of TCR from the 20th century tends to
9 be low biased compared to the model's true TCR.

10 2. Internal variability can push down or enhance the warming in ensemble members &
11 lead to large errors in TCR inferred from the 20th century.

12 3. We also verify that the details of the construction of the temperature dataset from
13 which TCR is inferred can lead to significant biases in TCR inferred from observed
14 warming.

15

16 **Plain language summary:**

17 The transient climate response (TCR) is defined to be the warming after 70 years of a 1% per
18 year increase in atmospheric CO₂. It is one of the important metrics in climate science because
19 it plays a key role in determining how much warming we will experience in the future. Previous
20 work has found that TCR inferred from observed warming over the 20th century tends to be
21 lower than TCR in climate models. This has been used by suggest that climate models are
22 overpredicting future warming. We use a large number of climate model runs to investigate
23 the methodology of this comparison. We find that TCR estimated from the 20th century
24 simulations may indeed be much lower than the model's true TCR. This arises from biases in
25 the methodology of estimating TCR from 20th century warming, as well as biases in the
26 construction of the observational temperature data sets. We therefore find no evidence that
27 models are overestimating TCR.

28

29 **Abstract**

30 The transient climate response (TCR), defined to be the warming in near-surface air
31 temperature after 70 years of a 1% per year increase in CO₂, can be estimated from observed
32 warming over the 19th and 20th centuries. Such analyses yield lower values than TCR estimated
33 from global climate models (GCMs). This disagreement has been used to suggest that GCMs'
34 climate may be too sensitive to increases in CO₂. Here we critically evaluate the methodology
35 of the comparison using a large ensemble of a fully coupled GCM simulating the historical
36 period, 1850–2005. We find that TCR estimated from model simulations of the historical period
37 can be much lower than the model's true TCR, replicating the disagreement seen between
38 observations and GCM estimates of TCR. This suggests that the disagreement could be
39 explained entirely by the details of the comparison and undercuts the suggestions that GCMs
40 overestimate TCR.

41 **Introduction**

42 The transient climate response (TCR) is frequently used to quantify the sensitivity of our climate
43 system to increases in greenhouse gases. It is defined to be the warming in near-surface air
44 temperature after 70 years of a 1% per year increase in atmospheric CO₂. As described below,
45 it can be estimated from observed warming over the 19th and 20th centuries, yielding most-
46 likely TCR values of 1.3-1.6 K [Bengtsson and Schwartz, 2013; Otto et al., 2013; Richardson et
47 al., 2016; Lewis and Curry, 2018]. These values lie below the CMIP5 ensemble average TCR of
48 1.8 K [Forster *et al.*, 2013]. This disagreement has been used to cast doubt on the fidelity of
49 model simulations of future climate change.

50 We will test the methodology of this comparison using a large model ensemble, an increasingly
51 popular tool to study the impact of internal variability on the climate system. The most
52 appropriate ensemble for this type of problem contains many runs of a single model with
53 identical physics and external forcing but different initial conditions. As each ensemble member
54 evolves in time, internal variability of the different members is out of phase, leading to
55 differences in the climate states among the ensemble members. In fact, one can think of our
56 observational record as one member of a theoretical ensemble of Earth's climate trajectories.

57 A model ensemble therefore gives us insight into what alternative climate histories may have
58 looked like.

59 **Data**

60 We analyze output from an ensemble of 100 runs of the fully-coupled Max Planck Institute
61 Earth System Model version 1.1 (MPI-ESM1.1) covering the period 1850-2005. The ensemble
62 was used by Dessler et al. [2018] to characterize the impact of internal variability on estimates
63 of the equilibrium climate sensitivity (ECS); they found that internal variability can lead to
64 significant errors in ECS inferred from historical observations. Hedemann et al. [2017] analyzed
65 this ensemble to determine potential causes of the so-called warming hiatus that occurred in
66 the 2000s.

67 As described by Dessler et al. [2018]: “This is the latest coupled climate model from the Max
68 Planck Institute for Meteorology and consists of the ECHAM6.3 atmosphere and land model
69 coupled to the MPI-OM ocean model. The atmospheric resolution is T63 spectral truncation,
70 corresponding to about 200 km, with 47 vertical levels, whereas the ocean has a nominal
71 resolution of about 1.5 degrees and 40 vertical levels. MPI-ESM1.1 is a bug-fixed and improved
72 version of the MPI-ESM used during CMIP5 [Giorgetta *et al.*, 2013] and nearly identical to the
73 MPI-ESM1.2 ... model being used to provide output to CMIP6, except that the historical forcings
74 are from the MPI-ESM. Each of the 100 members simulates the years 1850-2005 (Fig. 1) and
75 use the same evolution of historical natural and anthropogenic forcings. The members differ
76 only in their initial conditions —each starts from a different state sampled from a 2000-year
77 control simulation.”

78 Dessler et al. further say: “We calculate effective radiative forcing F for the ensemble by
79 subtracting top-of-atmosphere flux R in a run with climatological sea surface temperatures
80 (SSTs) and a constant pre-industrial atmosphere from average R from an ensemble of three
81 runs using the same SSTs but the time-varying atmospheric composition used in the historical
82 runs [Hansen *et al.*, 2005; Forster *et al.*, 2016]. The three-member ensemble begins with
83 perturbed atmospheric states. We estimate $F_{2\times\text{CO}_2}$ using the same approach in a set of fixed SST
84 runs in which CO_2 increases at 1% per year, which yields a $F_{2\times\text{CO}_2}$ value of 3.9 W/m^2 .”

85 We estimate $F_{2\times\text{CO}_2}$ using the same approach in a set of fixed SST runs, one with a pre-industrial
86 atmosphere and one in which CO_2 increases at 1% per year. We estimate $F_{2\times\text{CO}_2}$ as the average
87 difference in top-of-atmosphere flux over years 62-78, which produces a value of 3.7 W/m^2 .
88 This is lower than the value used in Dessler et al. [2018], 3.9 W/m^2 , which was estimated as
89 one-half of the average over years 130-150. We feel the value of 3.7 W/m^2 is a more
90 appropriate estimate of $2\times\text{CO}_2$ forcing in this model.

91 We will also analyze a 68-member ensemble of the MPI-ESM1.1 forced with CO_2 increasing at
92 1%/year (hereafter, “1% runs”). As with the historical ensemble, the 1% ensemble members
93 differ only in their initial conditions — each starts from a different state sampled from a 2000-
94 year pre-industrial control simulation.

95 **Analysis**

96 Time series of global-average near-surface air temperature for all 100 members are plotted in
97 Fig. 1 of Dessler et al. [2018]; that plot shows that the model ensemble is in good agreement
98 with observed surface temperatures. TCR can be estimated from the ensemble’s temperature
99 data with this equation [Gregory and Forster, 2008; Otto *et al.*, 2013; Richardson *et al.*, 2016]:

$$100 \quad \text{TCR}_{hist} = \Delta T \frac{F_{2\times\text{CO}_2}}{\Delta F} \quad (1)$$

101 where ΔT is the change in temperature over the historical period and ΔF is the change in
102 radiative forcing. In our analysis, Δ represents the change between the 1859-1882 average,
103 selected because it is not strongly influenced by volcanic eruptions [Mauritsen and Pincus,
104 2017; Lewis and Curry, 2018], and the average of the last ten years of the runs, 1996-2005. We
105 refer to TCRs estimated this way as TCR_{hist} .

106 We first calculate TCR_{hist} in each ensemble member using global-average near-surface air
107 temperature for ΔT . The calculated values range from 1.32 to 1.94 K (5-95% range 1.48-1.90 K)
108 (Fig. 1a, Table 1). The spread in these TCR estimates is entirely due to internal variability and
109 the spread is similar to previous estimates [Huber *et al.*, 2014; Hawkins *et al.*, 2016]. The
110 standard deviation of ΔT from the ensemble is 0.07 K, close to that assumed by Lewis and Curry
111 [2015], implying a similar spread in TCR in their analysis.

112 TCR is formally defined as the warming of global-average near-surface air temperature in
113 response to CO₂ increasing at 1% per year, at the time of doubling (year 70). This value, which
114 we will call TCR_{true}, can be estimated by averaging the warming (relative to pre-industrial) in
115 year 70 of the 68-member ensemble of 1% runs. We find that TCR_{true} for the MPI-ESM1.1 is
116 1.81 K; this is 0.13 K (7.6%) larger than the average of the ensemble's TCR_{hist} (1.68 K).

117 Thus, TCR_{hist} is a low-biased estimate of TCR_{true} in the ensemble. The magnitude, and even the
118 sign, of this bias varies depending on the portion of the historical record being examined (Table
119 1). Overall, though, we see a clear tendency for the TCR_{hist} to underestimate TCR_{true}. Previous
120 papers have suggested that the biases in TCR_{hist} could be due to aerosol forcing efficacy
121 [Kummer and Dessler, 2014; Shindell, 2014; Marvel *et al.*, 2015], although that explanation
122 remains to be validated in this ensemble.

123 We are now in a position to critically evaluate previous comparisons of TCR from observations
124 and GCMs. TCR estimated from observations, which are TCR_{hist}, have most-likely values in the
125 range 1.3-1.6 K [Bengtsson and Schwartz, 2013; Otto *et al.*, 2013; Richardson *et al.*, 2016; Lewis
126 and Curry, 2018], although the uncertainty in the individual estimates is large. The CMIP5
127 ensemble's TCR, which are TCR_{true}, fall in the range 1.8±0.6 K (average and 5-95% confidence
128 interval) [Forster *et al.*, 2013]. Our analysis of the MPI-ESM1.1 ensemble demonstrates how a
129 model with a TCR_{true} of 1.81 K might nevertheless produce TCR_{hist} in some ensemble members
130 that that are much lower (1.3-1.4, Figure 1a) and in agreement with observational estimates.
131 Thus, differences between observational TCRs and GCM TCRs could be mostly or entirely due to
132 these issues.

133 We can also confirm previous suggestions that two issues with the observed ΔT, masking and
134 blending, are further biasing TCR_{hist} to even lower values [Richardson *et al.*, 2016]. Masking
135 refers to the fact that the observations are geographically incomplete, and that the degree of
136 incompleteness has changed over time, leading to biases in global-average ΔT [Cowtan and
137 Way, 2014]. To test the impact of this on TCR_{hist}, we also calculated ΔT in the ensemble using a
138 time-varying mask derived from HadCRUT4 (v4.6.0.0) [Morice *et al.*, 2012]. Using this masked
139 ΔT in Eq. 1, ensemble average TCR_{hist} drops from 1.68 K to 1.59 K (Fig. 1b, Table 2).

140 The second issue is blending, which refers to the fact that observed ΔT data sets are usually a
141 blend of near-surface air temperature over land and sea ice but sea surface temperature (SST)
142 over open ocean. Because near-surface air temperature is warming faster than SSTs, this
143 blending lowers ΔT compared to an estimate derived entirely from near-surface air
144 temperature [Cowtan *et al.*, 2015; Santer *et al.*, 2000]. We test this by calculating a blended ΔT
145 in the ensemble, which we also mask following HadCRUT4. Using this blended and masked ΔT ,
146 ensemble average TCR_{hist} drops to 1.47 K (Fig. 1d, Table 2). Importantly, none of the individual
147 ensemble members have TCR_{hist} as large as the model's TCR_{true} .

148 Finally, we have also calculated blended ΔT using the temperature of the model's top ocean
149 layer (representing the top 12 m of the ocean) instead of SST. Using that estimate of ΔT , TCR_{hist}
150 drops even further, to an ensemble average of 1.44 K (Fig. 2f, Table 2).

151 **Conclusions**

152 We have investigated why observation-based estimates of TCR tend to be lower than those
153 from GCMs using a perfect model experiment. We have quantified a number of biases that can
154 explain most, if not all, of the disagreement: 1) a bias between TCR_{hist} and TCR_{true} , 2) a bias due
155 to incomplete spatial coverage in the observational ΔT record, and 3) a bias due to the
156 observational ΔT values being blends of air temperature and SSTs. These three biases are all
157 acting in the same direction, to push TCR_{hist} to lower values. The impact of internal variability,
158 which can suppress warming in some members of the ensemble, thereby further reducing
159 TCR_{hist} , is not yet quantifiable. But it has a potentially large magnitude and therefore could also
160 be playing a role in the model-observation difference.

161 The uncertainty in individual estimates of TCR_{hist} from observations are large and the range
162 easily covers most of the TCR_{true} values from the CMIP5 ensemble [Lewis and Curry, 2015; Lewis
163 and Curry, 2018; Richardson *et al.*, 2016]. Because of the large uncertainty in other parameters
164 (e.g., aerosol forcing), adding uncertainty due to the issues we discuss in this paper will produce
165 only nominal increases in the total uncertainty of the observational estimates. However, the
166 biases we have investigated are capable of explaining most or all of the disagreement between
167 the central values of the estimates, which has been the focus of much of the discussion.

168 Our work also informs how future analyses should be done. First, analyses should account for
169 the role of internal variability, most likely by comparing observations to an ensemble of runs. In
170 addition, we should not compare TCR_{hist} derived from observations to TCR_{true} — unless one can
171 quantify and adjust for the bias between these methods. A better approach would be to
172 compare TCR_{hist} from observations to TCR_{hist} derived from an ensemble of runs of the GCMs
173 covering the same period as the observations. Finally, one must account for biases in the
174 observations of ΔT due to masking and blending, most likely by calculating masked and blended
175 ΔT fields from the model and using those to estimate the model-derived TCR_{hist} .

176

177 **Acknowledgments:** This work was supported by NSF grant AGS-1661861 to Texas A&M
178 University. We thank the Bjorn Stevens, Thorsten Mauritsen, and Chris Hedemann of the Max-
179 Planck-Institut für Meteorologie for their help interpreting output from the ensemble that
180 formed the basis of this analysis. We also thank Mark Richardson for his suggestions on the
181 manuscript. Data and code are available from [insert link after paper is accepted and code is
182 finalized].

183

184 **References**

- 185 Bengtsson, L., & S. E. Schwartz (2013), Determination of a lower bound on Earth's climate
186 sensitivity, *Tellus B: Chemical and Physical Meteorology*, 65, 21533, doi:
187 10.3402/tellusb.v65i0.21533.
- 188 Cowtan, K., & R. G. Way (2014), Coverage bias in the HadCRUT4 temperature series and its
189 impact on recent temperature trends, *Q. J. R. Meteor. Soc.*, 140, 1935-1944, doi:
190 doi:10.1002/qj.2297.
- 191 Cowtan, K., Z. Hausfather, E. Hawkins, P. Jacobs, M. E. Mann, S. K. Miller, et al. (2015),
192 Robust comparison of climate models with observations using blended land air and
193 ocean sea surface temperatures, *Geophys. Res. Lett.*, 42, 6526-6534, doi:
194 10.1002/2015GL064888.
- 195 Dessler, A. E., T. Mauritsen, & B. Stevens (2018), The influence of internal variability on
196 Earth's energy balance framework and implications for estimating climate sensitivity,
197 *Atmos. Chem. Phys.*, 18, 5147-5155, doi: 10.5194/acp-18-5147-2018.
- 198 Forster, P. M., T. Andrews, P. Good, J. M. Gregory, L. S. Jackson, & M. Zelinka (2013),
199 Evaluating adjusted forcing and model spread for historical and future scenarios in the
200 CMIP5 generation of climate models, *Journal of Geophysical Research: Atmospheres*,
201 118, 1139-1150, doi: 10.1002/jgrd.50174.

202 Forster, P. M., T. Richardson, A. C. Maycock, C. J. Smith, B. H. Samset, G. Myhre, et al. (2016),
203 Recommendations for diagnosing effective radiative forcing from climate models for
204 CMIP6, *J. Geophys. Res.*, 121, 12460-12475, doi: 10.1002/2016jd025320.
205 Giorgetta, M. A., J. Jungclaus, C. H. Reick, S. Legutke, J. Bader, M. Böttinger, et al. (2013),
206 Climate and carbon cycle changes from 1850 to 2100 in MPI-ESM simulations for the
207 Coupled Model Intercomparison Project phase 5, *Journal of Advances in Modeling Earth*
208 *Systems*, 5, 572-597, doi: 10.1002/jame.20038.
209 Gregory, J. M., & P. M. Forster (2008), Transient climate response estimated from radiative
210 forcing and observed temperature change, *J. Geophys. Res.*, 113, doi:
211 10.1029/2008jd010405.
212 Hansen, J., M. Sato, R. Ruedy, L. Nazarenko, A. Lacis, G. A. Schmidt, et al. (2005), Efficacy of
213 climate forcings, *Journal of Geophysical Research: Atmospheres*, 110, doi:
214 10.1029/2005JD005776.
215 Hawkins, E., R. S. Smith, J. M. Gregory, & D. A. Stainforth (2016), Irreducible uncertainty in
216 near-term climate projections, *Climate Dynamics*, 46, 3807-3819, doi: 10.1007/s00382-
217 015-2806-8.
218 Hedemann, C., T. Mauritsen, J. Jungclaus, & J. Marotzke (2017), The subtle origins of
219 surface-warming hiatuses, *Nature Clim. Change*, 7, 336-339, doi:
220 10.1038/nclimate3274.
221 Huber, M., U. Beyerle, & R. Knutti (2014), Estimating climate sensitivity and future
222 temperature in the presence of natural climate variability, *Geophys. Res. Lett.*, 41, 2086-
223 2092, doi: 10.1002/2013GL058532.
224 Kummer, J. R., & A. E. Dessler (2014), The impact of forcing efficacy on the equilibrium
225 climate sensitivity, *Geophys. Res. Lett.*, 41, 3565-3568, doi: 10.1002/2014gl060046.
226 Lewis, N., & J. A. Curry (2015), The implications for climate sensitivity of AR5 forcing and
227 heat uptake estimates, *Climate Dynamics*, 45, 1009-1023, doi: 10.1007/s00382-014-
228 2342-y.
229 Lewis, N., & J. Curry (2018), The impact of recent forcing and ocean heat uptake data on
230 estimates of climate sensitivity, *J. Climate*, doi: 10.1175/jcli-d-17-0667.1.
231 Marvel, K., G. A. Schmidt, R. L. Miller, & L. S. Nazarenko (2015), Implications for climate
232 sensitivity from the response to individual forcings, *Nature Climate Change*, 6, 386, doi:
233 10.1038/nclimate2888.
234 Mauritsen, T., & R. Pincus (2017), Committed warming inferred from observations, *Nature*
235 *Climate Change*, 7, 652-655, doi: 10.1038/nclimate3357.
236 Morice, C. P., J. J. Kennedy, N. A. Rayner, & P. D. Jones (2012), Quantifying uncertainties in
237 global and regional temperature change using an ensemble of observational estimates:
238 The HadCRUT4 data set, *J. Geophys. Res.*, 117, doi: 10.1029/2011jd017187.
239 Otto, A., F. E. L. Otto, O. Boucher, J. Church, G. Hegerl, P. M. Forster, et al. (2013), Energy
240 budget constraints on climate response, *Nature Geoscience*, 6, 415-416, doi:
241 10.1038/ngeo1836.
242 Richardson, M., K. Cowtan, E. Hawkins, & M. B. Stolpe (2016), Reconciled climate response
243 estimates from climate models and the energy budget of Earth, *Nature Clim. Change*, 6,
244 931-935, doi: 10.1038/nclimate3066.
245 Santer, B. D., T. M. L. Wigley, D. J. Gaffen, L. Bengtsson, C. Doutriaux, J. S. Boyle, et al. (2000),
246 Interpreting differential temperature trends at the surface and in the lower
247 troposphere, *Science*, 287, 1227.

248 Shindell, D. T. (2014), Inhomogeneous forcing and transient climate sensitivity, Nature
249 Climate Change, 4, 274, doi: 10.1038/nclimate2136.
250

251
252

Table 1. TCR_{hist} calculated with different base and end periods

base period	end period	average (K)	Full TCR range (K)	5-95% TCR range (K)	width (K)	% diff from true TCR	ΔF (W/m ²)
1859-1882	1940-1949	1.82	0.63-2.88	1.15-2.50	1.35	0.4	0.54
1859-1882	1951-1960	1.96	1.10-3.13	1.32-2.67	1.34	7.6	0.59
1859-1882	1969-1978	1.71	1.01-2.91	1.24-2.24	0.99	-5.8	0.81
1859-1882	1996-2005	1.68	1.32-1.94	1.48-1.90	0.42	-7.7	1.85
1930-1939	1996-2005	1.65	0.97-2.07	1.35-1.99	0.64	-9.7	1.41
1940-1949	1996-2005	1.62	1.02-2.16	1.28-2.04	0.76	-11.5	1.31
1951-1960	1996-2005	1.55	0.91-2.04	1.20-1.90	0.70	-16.8	1.26
1970-1979	1996-2005	1.67	0.99-2.42	1.20-2.09	0.90	-8.5	0.99

253 The bold line is the case primarily discussed in the text. Width is the difference between the 5th and 95th
254 percentile values; % difference is average TCR_{hist} minus TCR_{true}, 1.81 K, divided by average TCR_{hist}, in
255 percent; ΔF is the change in forcing between the base and end periods.

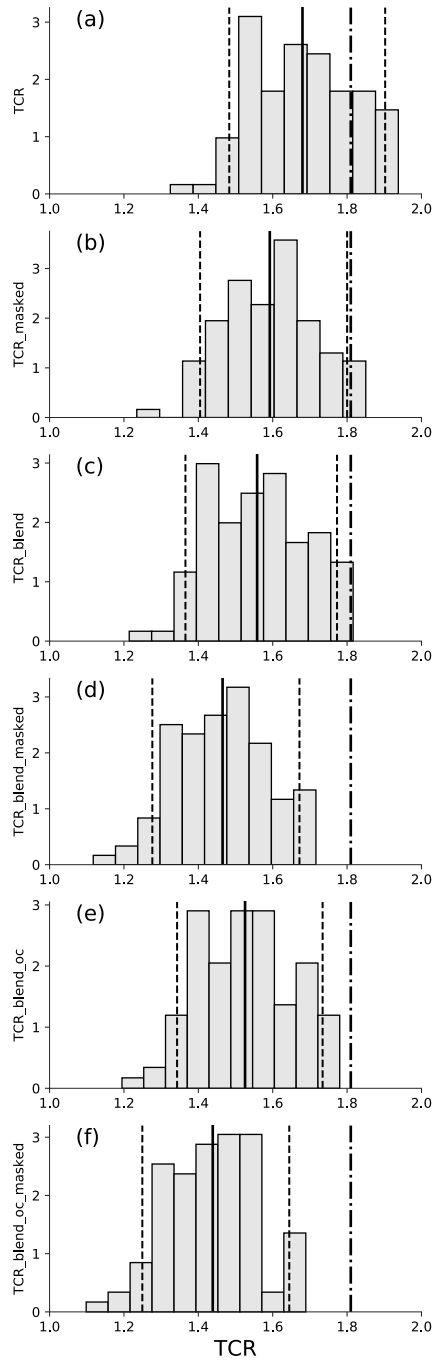
256
257

Table 2. TCR_{hist} calculated with different versions of ΔT

ΔT _s		average (K)	5-95% TCR range (K)	% diff from True TCR
TCR	ΔT is global-average near-surface air temperature	1.68	1.48-1.90	-7.7
TCR_masked	Same as TCR, but geographic coverage follows HadCRUT4	1.59	1.40-1.80	-13.7
TCR_blend	ΔT is a blend of near-surface air temperature over land and sea ice and SSTs over open ocean	1.56	1.37-1.77	-16.2
TCR_blend_masked	Same as TCR_blend, but geographic coverage follows HadCRUT4	1.47	1.28-1.67	-23.5
TCR_blend_oc	ΔT is a blend of near-surface air temperature over land and sea ice; elsewhere, use temperature of the top 12 m of the ocean	1.53	1.34-1.73	-18.6
TCR_blend_oc_masked	Same as TCR_blend_oc, but geographic coverage follows HadCRUT4	1.44	1.25-1.64	-25.8

258 The bold line is the base case primarily discussed in the text; % difference is average TCR_{hist} minus
259 TCR_{true}, 1.81 K, divided by average TCR_{hist}, in percent.

260
261



262

263 Figure 1. Histograms of TCR_{hist} (K) from the ensemble. Each panel shows the calculation with a
264 different version of ΔT ; see Table 2 for definitions. The solid black line represents the average,
265 the dashed lines are the 5th and 95th percentiles. The dot-dashed line is TCR_{true} of the model,
266 1.81 K.